

Influence of MgO overlayers on the electronic states of bct Co(001) thin films grown on bcc Fe(001)/GaAs(001)

Liu-Niu Tong* and Cai-Lian Deng

Institute of Material Science and Engineering, Anhui University of Technology, Ma-An-Shan, 243002, Anhui, China

Frank Matthes, Martina Müller, and Claus M. Schneider

Institute of Solid State Research, Research Centre Jülich, D-52425 Jülich, Germany

and Leibnitz-Institute for Solid State and Materials Research Dresden, Helmholtzstrasse 20, 01069 Dresden, Germany

Chan-Gyu Lee

School of Nano and Advanced Materials Engineering, Changwon National University, 9 Sarim-dong, Changwon, Gyeongnam, 641-773, Korea

(Received 8 October 2005; revised manuscript received 9 January 2006; published 1 June 2006; corrected 19 June 2006)

The spin polarization of the valence band electronic states of strained bcc Co(001) and MgO/Co(001) thin films grown onto a bcc Fe(001) seed layer on GaAs(001) are investigated by employing spin-resolved photoemission spectroscopy. The experimental results are compared with the calculated energy band structure of bcc and bct Co(001), and discussed in the framework of the interband transition model, which allows one to ascribe the observed spectral features to bands of given spin and spatial symmetry. In contrast to the positive spin polarization observed at the MgO/Fe(001) interface, a large negative spin polarization of the electronic states at the Fermi level is observed for the MgO/Co/Fe/GaAs(001) system. Such a large negative spin polarization is attributed to a change in the energy band structure at the bct Co/bcc Fe(001) interface.

DOI: [10.1103/PhysRevB.73.214401](https://doi.org/10.1103/PhysRevB.73.214401)

PACS number(s): 75.47.Jn, 85.70.Kh, 73.40.Gk, 68.55.Jk

I. INTRODUCTION

A new area of condensed matter physics called spintronics that utilizes the spin degree of freedom of the charge carriers has developed rapidly over the last few years. Magnetic tunnel junctions (MTJs) consisting of two ferromagnetic electrodes separated by an insulating layer exhibits magnetoresistance at room temperature. This tunnel magnetoresistance (TMR) effect has applications for magnetoresistive random access memory (MRRAM) and magnetic sensors.^{1,2} MRRAM is expected to be a unified memory device having desirable technological advancements such as increased processing speed, decreased power consumption, greater integration densities, and most important, nonvolatility. Much of the early spintronics research has focused on MTJ systems with amorphous aluminum oxide tunneling barriers and ferromagnetic transitional metal (FM) electrodes as a source of spin polarized carriers. However, the theoretical treatments are most often based on single-crystalline model systems. This makes it difficult for one to identify the prominent mechanisms from the many factors that influence the TMR, such as band structure, interfacial bonding, structural disorder, and interface roughness.^{3,4} In MTJs with an amorphous barrier, electron tunneling is dominated by noncoherent tunneling and the TMR effect can be simply described by the effective spin polarization of the magnetic electrodes. The maximum of the observed TMR ratio is about 70% for the MTJs with polycrystalline FM electrodes and an amorphous barrier.⁵ Thus the scope for significantly improving the TMR ratio of MTJs with amorphous barriers is very limited. Recently an epitaxial single crystalline Fe/MgO/Fe system, as a quasiperfect model of MTJs systems, has attracted great

interest due to its almost perfect lattice match and possible high performance of MTJs.^{6,7} The theoretical predication for the TMR value of a single crystal Fe/MgO/Fe(001) MTJ with an ideal interface is larger than 1000%.^{8,9} The origin of the high TMR ratio in single crystal MTJs is not the diffusive tunneling of Julliere's model but the coherent spin-polarized tunneling in epitaxial MTJ. A recent experimental result of the highest TMR ratio on the Fe/MgO/Fe(001) system is about 146% at $T=20$ K,¹⁰ showing the likelihood of a coherent spin-polarized tunneling effect, although it is still lower than the value of the theoretical predication or the value observed in other MTJ systems. For example, a TMR ratio of 220% at RT has been achieved recently in the MTJs with a structure of FeCo(001)/MgO(001)/Co₅₆Fe₂₄B₂₀.¹¹

The high TMR effect amplitude is largely determined by the electronic structure of the whole MTJs including the spin properties at interfaces between the FM electrode and the oxide barrier. Although some previous works have been done in order to investigate the electronic structure at FM/Oxide barrier interfaces, the nature of the interfacial electronic structure and its role on the spin-polarized tunneling effect of MTJs are not well understood yet.^{12–15} With regard to the critical importance of interface properties, especially in a spin-dependent electronic structure, in understanding the spin-polarized tunneling behavior of MTJs, we have explored the spin polarization of the valence band electronic structure at the interface of MgO/Co(001) films employing spin- and angle-resolved normal photoemission spectroscopy (SARPS). Our choice of this MgO/Co(001) system is motivated by the following considerations. First, the bcc phase of Co electrodes for magnetoresistive devices is desired to investigate the influence of the physical and electronic struc-

ture on TMR. Recently Zhang and Butler predicted that the TMR of bcc Co(001)/MgO(001)/Co(001) of TMJs can be several times larger than the very large TMR predicted for the Fe/MgO/Fe system.¹⁶ The origin of this large TMR effect can be understood by considering the coherent tunneling of the electrons at the Fermi energy traveling perpendicular to the interfaces. For the minority spins there is no state with Δ_1 symmetry whereas for the majority spins there is only a Δ_1 state. Within the MgO barrier the Δ_1 state decays much more slowly than the other states. In order to better understand the mechanism of the TMR effect and to test the theoretical predication, it is now appropriate to experimentally explore the electronic structure of the bcc Co(001) thin film and the spin properties at the MgO/Co(001) interface. To our knowledge, there is no spin-resolved photoemission spectroscopy study of the valence band electronic structure of bcc Co(001) film available in the literature up to now. Secondly, in the experimental aspect, a thin Co film with a bcc phase can also be stabilized under special conditions. The first report of the bcc Co, made by Prinz, used growth on GaAs(110).¹⁷ Later, bcc Co was stabilized inbetween Fe layers and Cr layers.^{18,19} However, it should be kept in mind that although early calculations predicted bcc Co to be a metastable phase, more recent papers showed that the bcc phase is unstable against volume-conserving tetragonal distortions and the true metastable phase is a body-centered tetragonal (bct) phase, with a c/a ratio of 0.92, where c is the lattice constant in the growth direction and a is the lattice constant in the plane perpendicular to the growth direction.^{20,21} It is noted that in the literature one still uses the expression of bcc Co even when the layer is strained ($c/a \neq 1$) because both bcc and bct Co are, in practice, strain-induced phases and all grown layers show some strain and distortions.²² In this paper we systematically investigate the spin polarization of the electronic states at the MgO/Co/Fe(001) magnetic tunneling junction interface and find that the change in the energy band structure at the bct Co/bcc Fe(001) interface results in a large negative spin polarization at the Fermi level of the MgO/Co/Fe/GaAs(001) system. Our photoemission results of larger spin polarization of the MgO/bct Co(001) system than that of the MgO/bcc Fe(001) interface is consistent with first-principles calculations¹⁶ and recent large TMR observations on MTJs of the bcc Co(001)/MgO/Fe system.³⁰

II. EXPERIMENTAL DETAILS

In order to induce bcc or tetragonally distorted bcc (known as bct) Co(001) film a 15 ML Fe(001) seed layer was first deposited on a Ga terminated GaAs(001)-(4 \times 6) surface by using molecular beam epitaxy. The Ga-terminated GaAs(001)-(4 \times 6) surface is favored in order to be able to suppress the As segregation on the Fe surface and to improve the epitaxial growth of Fe(001). Figure 1 shows low energy electron diffraction (LEED) patterns of the GaAs(001)-(4 \times 6) surface as well as the bcc Fe(001) and Co(8 ML)/Fe(15 ML) on GaAs(001). The LEED images of Fe surface [Figs. 1(b) and 1(c)] show good crystallinity and

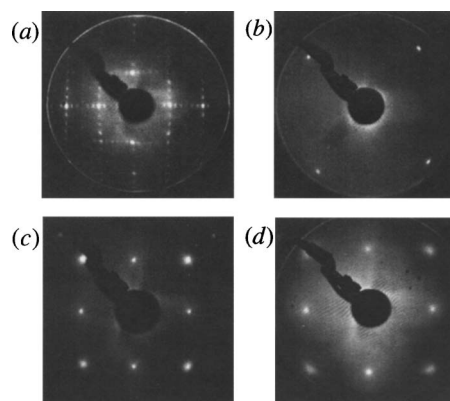


FIG. 1. LEED pattern of (a) GaAs(001)-4 \times 6, $E=113$ eV; (b) 15 ML Fe/GaAs(001), $E=38$ eV; (c) 15 ML Fe/GaAs(001), $E=187$ eV; (d) 8 ML Co/15 ML Fe/GaAs(001), $E=172$ eV.

flatness of the epitaxial Fe(001). On such a fine quality Fe(001) surface 8 ML Co thin film was grown in a tetragonally distorted bcc (bct) phase as shown in Fig. 1(d). The increase of the background intensity for the Co/Fe/GaAs(001) LEED image indicates the presence of some roughness and strain-induced distortion of all grown layers of bct Co at the Co/Fe(001) interface because of a different in-plane lattice constant between bcc Fe (0.286 nm) and bcc Co (0.282 nm). The increase of the background intensity after growing Co on bcc Fe(001) is in agreement with previous work on this system.¹⁹

The MgO films were grown by electron-beam evaporation from an Mg rod and simultaneous oxidation in an oxygen partial pressure of 1×10^{-8} mbar, whereby the oxygen is guided through a nozzle directly to the sample surface. The success of the oxidation procedure was verified by comparing the Auger electron spectrum of the oxidized Mg film with a reference taken from an MgO crystal surface. The MgO evaporation rate was calibrated by determining the attenuation of the Cu LMM Auger transition as described in Ref. 23. The thickness of the MgO barrier in the paper always means a nominal thickness. The possibility of the oxidation of Co-layers during the preparation of the MgO overlayers on it has also been taken into consideration and has been checked via the following: First we exposed the clean Co/Fe/GaAs(001) surface to the oxygen with the same oxygen partial pressure 1×10^{-8} mbar as used preparing the MgO films. The exposure time was as long as the period of evaporation of 2 ML MgO film. Afterwards, we pumped the chamber into an ultrahigh vacuum condition again and then checked the surface of Co/Fe/GaAs(001) film by Auger and LEED measurements. However, no oxygen signal was observed within the experimental error range. After growing MgO overlayers on the Co/Fe/GaAs(001) surface, the Auger measurements showed no significant peak shift of the Co signal, indicating the Co layers were hardly affected by exposure to oxygen with such a low partial pressure during preparation of MgO on it.

The magnetic properties were characterized by *in situ* longitudinal magneto-optical Kerr effect (MOKE) measurements. The pure 15 ML Fe/GaAs(001) thin film showed a

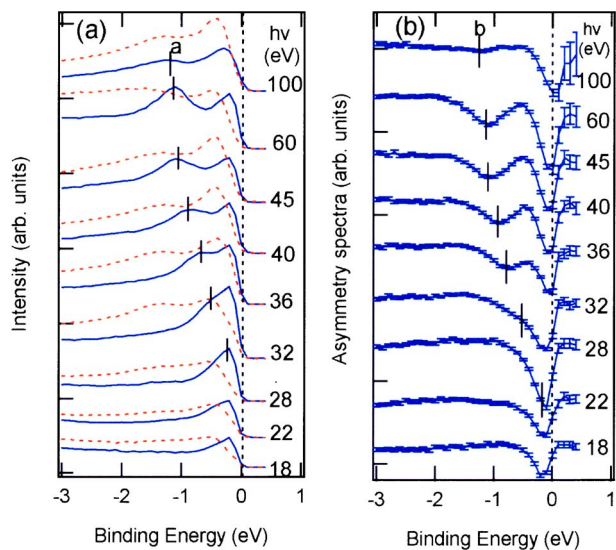


FIG. 2. (Color online) (a) The experimental majority (dashed line) and minority (solid line) normal photoemission spectra from 8 ML Co(001) on 15 ML Fe film grown on GaAs(001). (b) The corresponding asymmetry spectra at photon energies as indicated in the figure.

strong uniaxial anisotropy with easy axis oriented along a $[110]$ direction, which is consistent with previous reports in the literature.^{24–27} After growing 8 ML Co on Fe(001), the MOKE measurements showed a similar behavior to that of Fe film on GaAs(001) with only a slight increase of the coercive field for the Co/Fe/(001)GaAs(001) film, indicating that there is a strong exchange coupling between Co and Fe layers. The spin- and angle-resolved photoemission spectroscopy (SARPS) experiments were performed at the undulator beam line U-125-1 PGM (BESSY). The incident linearly P -polarized light made an angle of 45° with the normal surface. The experiments were done in magnetic remanence with the sample magnetized along the in-plane $[110]$ direction, which corresponds to the easy axis for these Co/Fe(001) thin films grown on GaAs(001). The photoelectrons were detected along the normal surface. The energy of the photoelectrons was determined using a cylindrical mirror type analyzer with an integrated LEED spin-polarization detector (CSA200-SPLEED combination). The asymmetry spectra were recorded for opposite magnetization directions to eliminate the apparatus asymmetry. The spin polarization P was calculated from the experimental asymmetry using a spin sensitivity of $S=0.23$. From the total intensity I_0 and the spin polarization P , the partial intensities I_+ and I_- with spin-up and spin-down character were derived according to $I_+=I_0/2(1+P)$ and $I_-=I_0/2(1-P)$. The overall energy resolution defined by the spectral resolution of the beam line, the angular acceptance of the entrance electron optics (6°), pass energy of the analyzer, and slit width is nominally 200 meV. All of the measurements were made at room temperature.

III. EXPERIMENTAL RESULTS

A. Co/Fe/GaAs(001)

Figure 2(a) shows spin-resolved normal photoemission

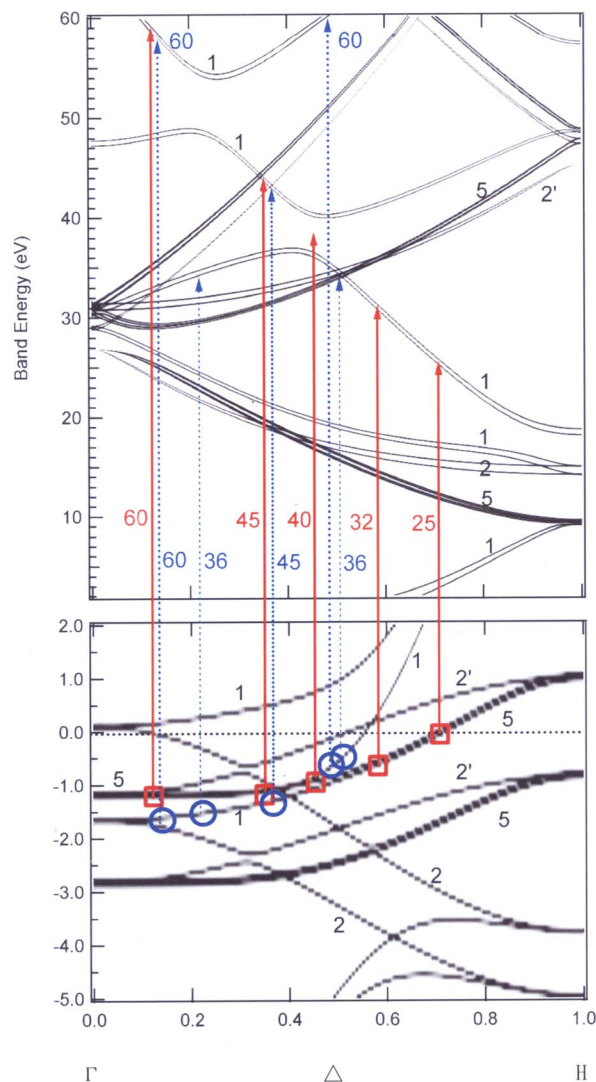


FIG. 3. (Color online) The calculated energy band structure of bcc Co(001) along Γ - H line. Some representative direct transitions from initial states on Δ_5^\downarrow symmetry and Δ_1^\uparrow symmetry to the corresponding final states are suggested by perpendicular solid arrows and dashed arrows, respectively, at photon energies indicated next to the arrows. The horizontal dashed line is referred to the Fermi level.

spectra recorded from 8 ML clean Co thin film on a 15 ML Fe(001) seed layer grown on GaAs(001) at several photon energies from $h\nu=18$ to 100 eV. The corresponding asymmetry spectra are also shown in Fig. 2(b). In order to analyze our data, we have performed a spin-polarized fully relativistic Korringa-Kohn-Rostocker band structure calculation for bulk bcc Co(001) using the Munich SPRKKR package.²⁸ Figure 3 shows the results of this calculation. At normal emission, the dipole selection rules allow direct transitions from the initial states of only Δ_1 and Δ_5 spatial symmetry into the final states with Δ_1 spatial symmetry. According to the direct transition model, the possible direct transitions from the initial bulk states to the corresponding final states (Δ_1 bands) at the experimental photon energies from $h\nu=18$ to 100 eV can thus be obtained. Figure 3 shows some

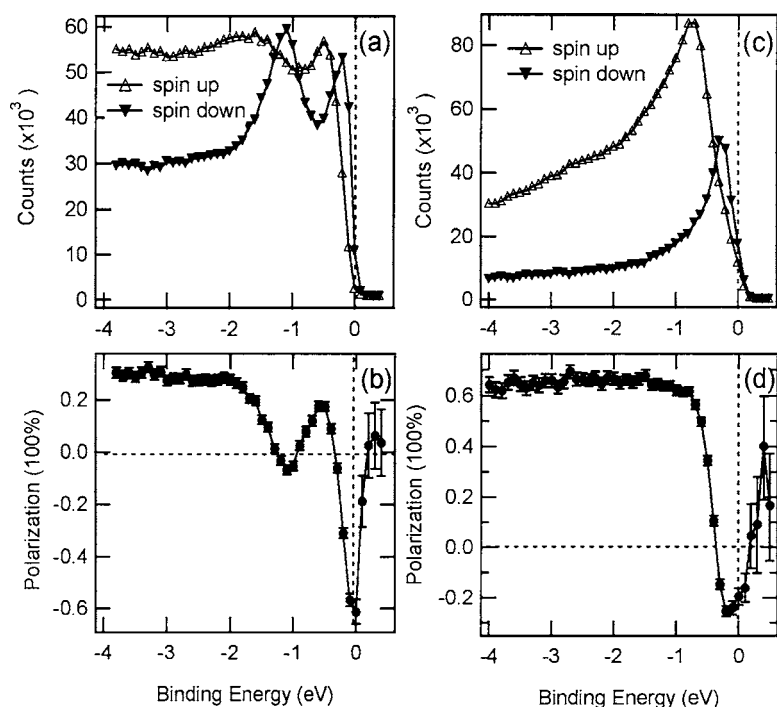


FIG. 4. The spin-resolved normal photoemission spectra of (a) Co(8 ML)/Fe(15 ML)/GaAs(001) and (c) Fe(15 ML)/GaAs(001) films, respectively, at 60 eV photon energy. (b) and (d) show the spin polarization spectra corresponding to the spectra of (a) and (c), respectively.

representative direct transitions from the initial states in minority Δ_5^\downarrow spatial symmetry (denoted by the square points) and in majority Δ_1^\uparrow symmetry (denoted by the circle points) to the corresponding final states as suggested by perpendicular solid and dashed arrows, respectively, at the photon energies indicated next to the arrows. The dependence of the binding energy of our measured minority peak “a” as indicated by a short line in Fig. 2(a) on the exciting photon energy is quite consistent with the energy band dispersion of calculated initial bulk states as indicated by the square points in the band of Δ_5^\downarrow symmetry as shown in Fig. 3. The minority peak “a” is located at the binding energy of $E_B = (1.2 \pm 0.2)$ eV for the spectrum at $h\nu = 60$ eV. With decreasing photon energy the peak “a” position gradually moves towards the Fermi level and crosses above it at a photon energy of about $h\nu = 25$ eV, at which the Δ_5^\downarrow band is also just across E_F as shown in Fig. 3. The intense minority peak “a” causes a significant feature of vale “b” in the corresponding asymmetry spectra as shown in Fig. 2(b). So, we ascribed this minority peak “a” to the direct transitions from the initial bulk states in Δ_5^\downarrow symmetry below the Fermi energy (E_F) level.

Besides peak “a” another intense spin-down peak near the Fermi level appears between 0.2 to 0.4 eV in almost all of the spectra collected using 0.2 eV resolution. This minority feature results in even deep vale near E_F on the corresponding asymmetry spectra as shown in Fig. 2(b). This observed spin-down feature near E_F is unexpected and hard to explain by the calculated bcc Co(001) band structure, which shows that for the minority spins there is no state with Δ_1 symmetry just below Fermi level, because the whole minority Δ_1 symmetry is just above E_F as shown in Fig. 3. Our calculation of the bcc Co(001) energy band structure is also in agreement with the result concluded by the first-principles calculations on a bcc Co/MgO/Co tunneling junction.¹⁶ Does this spin-

down feature near E_F come from the photoemission of an underlying Fe seed layer below 8 ML Co layers? The answer for this question is dependent on the different experimental photon energies. For example, at 100 eV of photon energy the escape depth of the photoelectrons is large enough to probe the Fe states below 8 ML Co layers. Thus at 100 eV of photon energy we cannot rule out some possible contribution from initial Fe states to our measured minority feature near E_F in the spectrum of the Co/Fe/GaAs(001) film. However, at 60 eV of photon energy the escape depth of photoelectrons through the material is equal to only a few angstroms. The measured spin-resolved photoemission spectra of the Co/Fe/GaAs(001) film is also completely different with the spectra of the clean Fe(001)/GaAs(001) film. Figure 4 shows the corresponding spectra of these two films measured with the same experimental conditions. It is noted that in the majority spectra of the Fe/GaAs(001) film an intense spin-up peak of Fe-states appears at 0.8 eV binding energy (E_B) with almost double the intensity of the spin-down Fe peak at $E_B = 0.2$ eV for the Fe(001) film as shown in Fig. 4(c). While in the majority spectrum of Co/Fe/GaAs(001) film, instead of a intense spin-up peak of Fe states at $E_B = 0.8$ eV, we measured a vale between the two majority peaks with a similar intensity of the minority peak at $E_B = 0.2$ eV below the Fermi level as shown in Fig. 4(a). From the following analysis we will see that these two spin-up peaks in the majority spectrum of the Co/Fe/GaAs(001) film could also be well explained as direct transitions from the initial states in the Δ_1^\uparrow symmetry of bcc Co(001). Our above experimental fact suggests that the features observed on the spectra of $h\nu = 60$ eV for the Co/Fe/GaAs(001) film are mainly originating from 8 ML Co(001) states and the Fe layer contribution to the signal is negligible.

As mentioned above the bcc Co phase is unstable against volume-conserving tetragonal distortions and the body-

centered tetragonal (bct) Co is more of a favorite structure because of the strain-induced distortion for Co thin film when Co is grown on bcc Fe(001). The energy band structure calculation of bct Co(001) has been performed by Duò and co-authors and it was shown in Fig. 1 of Ref. 29. Compared to the bcc Co(001) band structure, it was found that the energy band of bct Co(001) was shifted down slightly, resulting in partial states in the Δ_1^\downarrow symmetry around Γ point (about a quarter of Γ - H line of the bulk Brillouin zone) occupied just below Fermi energy. Based on the direct transition model and the band structure of bct Co(001), our observed minority feature appearing at the Fermi level in almost all of the spectra of Co/Fe(001) film could be well explained. It is interesting to note that at a photon energy of 60 eV the spectra shows larger spin-down intensity compared to that at other photon energies. This phenomenon is consistent with the energy band dispersion of the minority Δ_1^\downarrow symmetry near E_F of the calculated bct Co(001), which shows that more states in the Δ_1^\downarrow symmetry are occupied around the Γ point and along Γ - H line of the bulk Brillouin zone the occupied minority states become less when the Δ_1^\downarrow band gradually moves away and goes above the Fermi level. At 100 eV, the spectra show less spin-down intensity and larger spin-up intensity compared to the spectra at a photon energy of 60 eV. This phenomenon is partially related to an additional photoemission with larger spin-up intensity contributed from the lower Fe-layer of the Co/Fe/GaAs(001) film, because at 100 eV the escape depth of the photoelectrons is large enough to get the signal from the lower Fe-layers. Besides, at 100 eV of photon energy the angle integrates a large part of the Brillouin zone by using a six degree of acceptance angle and thus it may result in more spin-up intensity and less spin-down intensity at the Fermi level.

Now, let us turn to the spin-up features observed on the majority spectra of the Co/Fe/GaAs(001) film. On the majority spectra there are two broad features observed within our experimental binding energy. One of them is located at binding energy $E_B=(0.5\pm 0.2)$ eV, and another broad feature is located at $E_B=(1.4\pm 0.2)$ eV below the Fermi level. Both features show only a weak photon energy dependence. The dispersion of spin-up spectra is so different from spin-down spectra. However, spin-up spectra can also be well explained based on the calculated bcc or bct Co(001) band structure within the direct transition model. According to the direct transition model some representative transitions from initial bulk states in the majority Δ_1^\uparrow symmetry are indicated in Fig. 2 by perpendicular dashed arrows for some experimental photon energies of $h\nu=36, 45,$ and 60 eV, respectively. It is noted that for some excitation photon energies there are two possible transitions originating from different initial states in the Δ_1^\uparrow symmetry corresponding to the same photon energy. In other words, among all of these possible transitions, the initial bulk states in Δ_1^\uparrow symmetry can be classified into two sets. Each set consists of several very close initial states in the Δ_1^\uparrow symmetry, i.e., one of them is within the binding energy range of $E_B=(0.5\pm 0.2)$ eV, and the another is within $E_B=(1.4\pm 0.2)$ eV binding energy range. These two set transitions cause two broad spin-up features as shown in Fig. 2.

Figures 4(b) and 4(d) show the spin polarization spectra corresponding to the spectra of Figs. 4(a) and 4(c), respec-

tively. We define the spin polarization P as the difference between the partial intensities for majority and minority spins, normalized to the total intensity, $P=(I_{\text{up}}-I_{\text{down}})/(I_{\text{up}}+I_{\text{down}})$. It is interesting to find that the spin polarization spectra exhibit large spin polarization, $P=-(60\pm 5)\%$, at E_F for the Co/Fe/GaAs(001) system. This spin polarization value is about double that of the bcc Fe(001)/GaAs(001) film as shown in Fig. 4(d). In principle, the value of the spin polarization at E_F is determined by the energy band structure at the Fermi level, i.e., the imbalance between the density of states (DOS) for the majority and minority spin at the Fermi level. For the bct Co(001) band structure at Fermi level, the large band separation between Δ_1^\uparrow and Δ_1^\downarrow symmetries results in a large imbalance between the DOS for spin-up and spin-down electrons and therefore large spin polarization at the Fermi level. While for bcc Fe(001) band structure at Fermi energy, the narrow band separation between Δ_1^\uparrow and Δ_5^\downarrow symmetries results in a small imbalance between the DOS for spin-up and spin-down electrons and thus a small spin polarization at Fermi energy level. Besides strong direct exchange coupling between Co and the underlying Fe layers and strong uniaxial anisotropy as indicated from our MOKE measurements as mentioned above are also some possible factors that may increase our measured large spin polarization signal for the Co/Fe/GaAs(001) film. Our experimental observation of such a large spin polarization of the Co/Fe/GaAs(001) film compared to the bcc Fe(001)/GaAs(001) system is consistent with first-principles calculations¹⁶ and the recent large TMR observation on MTJs of bcc Co(001)/MgO/Fe system.³⁰

B. MgO/Co/Fe/GaAs(001)

Figures 5(a) and 5(c) show typical spin-resolved valence band photoemission spectra of the clean Co(8 ML)/Fe(15 ML)/GaAs(001) film and the MgO covered MgO(1 ML)/Co(8 ML)/Fe(15 ML)/GaAs(001) film, respectively, at photon energy of $h\nu=40$ eV. The spin polarization corresponding to the spectra of Figs. 5(a) and 5(c) is depicted in Figs. 5(b) and 5(d), respectively. It is shown that the MgO density of state (DOS) in the photoemission spectra starts around 3 eV below the Fermi level due to the insulating nature of MgO thin film, and in the $E_B < 3$ eV range the main photoemission features originating from the transitions of underlying Co/Fe/GaAs(001) film can be still seen. As a surprising finding, our spin-resolved measurements reveal a spin and symmetry dependent attenuation of the direct transitions from the Co/Fe(001) film upon MgO overlayer, i.e., the attenuation of the minority feature at $E_B=1$ eV, originating from direct transitions from initial bulk states in Δ_5^\downarrow symmetry, is stronger than one of the other features originating from the Δ_1 initial band upon MgO covering. This phenomenon can be still clearly reflected by comparing the spin polarization spectra of the Co/Fe/GaAs(001) film and the MgO/Co/Fe/GaAs(001) film as shown in Figs. 5(b) and 5(d), respectively. It is shown that with covering 1 ML MgO on the Co/Fe/GaAs(001) surface the vale at binding energy $E_B=1$ eV is almost completely smeared out, while the an-

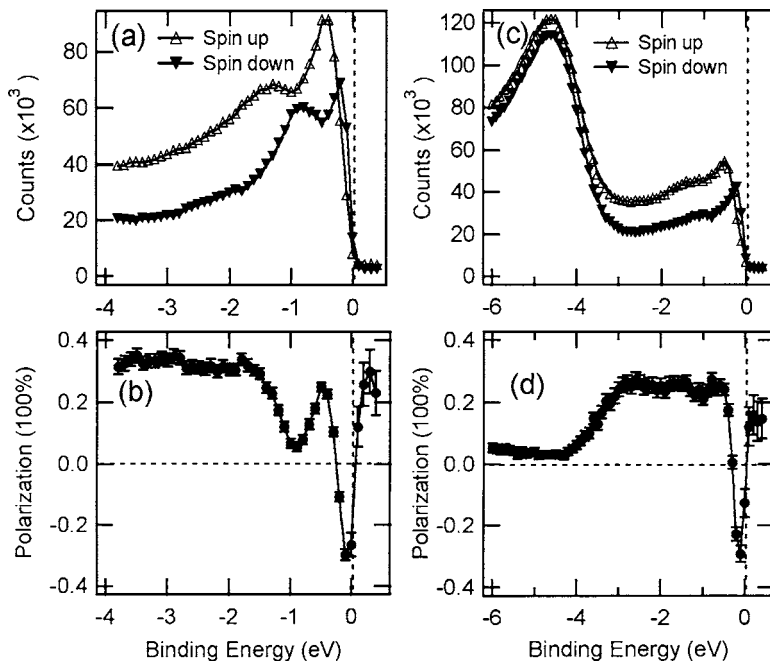


FIG. 5. The spin-resolved normal photoemission spectra of (a) clean Co(8 ML)/Fe(15 ML)/GaAs(001) film, and (c) MgO covered MgO(1 ML)/Co(8 ML)/Fe(15 ML)/GaAs(001) films at photon energy $h\nu=40$ eV; (b) and (d) are the spin polarization corresponding to the spectra of (a) and (c), respectively.

other dip just at the Fermi level is only slightly modified. A similar phenomenon of the spin and symmetry dependent modification of the electronic state upon the MgO overlayer was also observed in our previous published MgO/Fe(001) system by a spin-resolved photoemission spectra.³¹ Our SARPS data give clear experimental evidence that the stronger modification of the interface electronic states in Δ_5^\perp symmetry than the one in Δ_1 symmetry, is a common nature for tetragonally distorted bcc Co(001) and bcc Fe(001) surface when MgO is covered on it.

Figure 6(b) compiles the spin-resolved normal photoemission spectra at some typical photon energies as

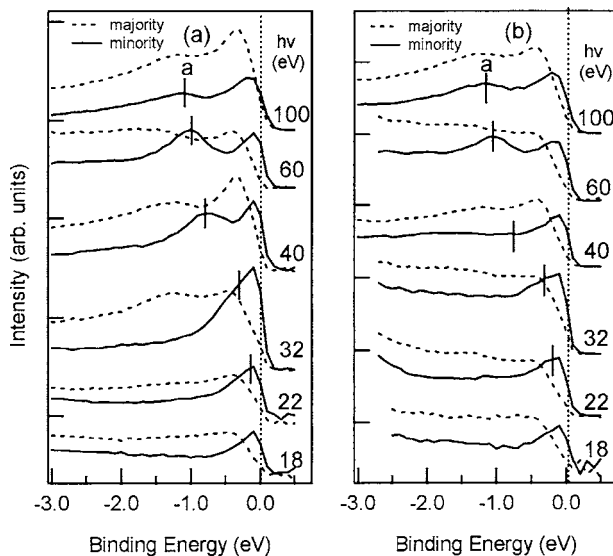


FIG. 6. The experimental majority (dashed line) and minority (solid line) normal photoemission spectra from (a) clean Co(8 ML)/Fe(15 ML)/GaAs(001) film, and (b) MgO(1 ML)/Co(8 ML)/Fe(15 ML)/GaAs(001) film at photon energies indicated in the figure.

indicated in the figure for MgO(1 ML)/Co(8 ML)/Fe(15 ML)/GaAs(001) film. For comparison purposes, the corresponding spectra of clean Co(8 ML)/Fe(15 ML)/GaAs(001) film are also shown in Fig. 6(a). It was shown that the spin and symmetry dependent attenuation of the photoelectrons from the MgO/Co/Fe/GaAs(001) film can also be seen on the spectra at photon energies of $h\nu=22, 32,$ and 60 eV, respectively. However, the weight decrease of the minority peak “a” is not as strong as that of the spectra at $h\nu=40$ eV. This observed photon energy dependent attenuation of the transitions from underlying $3d$ transition-metal may be related to the different escape depth of the photoelectrons for different photon energy and layer depth dependent modifications of the electronic structure of the MgO/Co/Fe(001) film. According to the universal curve the escape depth is just at the vale of the curve with the minimum about a few atomic planes for the photon energies around 40 to 60 eV. Within these photon energies, the measured features are dominated mainly by the direct transitions of the surfacial layer(s) of the film towards the vacuum. Especially at the photon energy of 40 eV the measured feature is very surface sensitive because a final state band gap exists between the band energy $E_{\text{Band}}=37$ eV and 40 eV above the Fermi level as shown in Fig. 3. It is the most surface sensitive to probe the electronic state modification through atom bonding at the MgO/Co(001) interface by using photon energies around 40 to 60 eV. At a photon energy of 100 eV, the spectra show only weak modification upon MgO overlayers, indicating the measured features at 100 eV are dominated by the photon electrons from the deep layers of MgO/Co/Fe/GaAs(001) film and the electronic structure of deep layers are almost not affected. The above experimental data suggest that upon MgO overlayers on the Co/Fe/GaAs(001) film the interface electronic state, especially in a minority Δ_5^\perp symmetry, involved at MgO/Co(001) interface is strongly modified through interfacial atom bonding between Co and MgO, while the electronic states in Δ_1 symmetry and deep layers

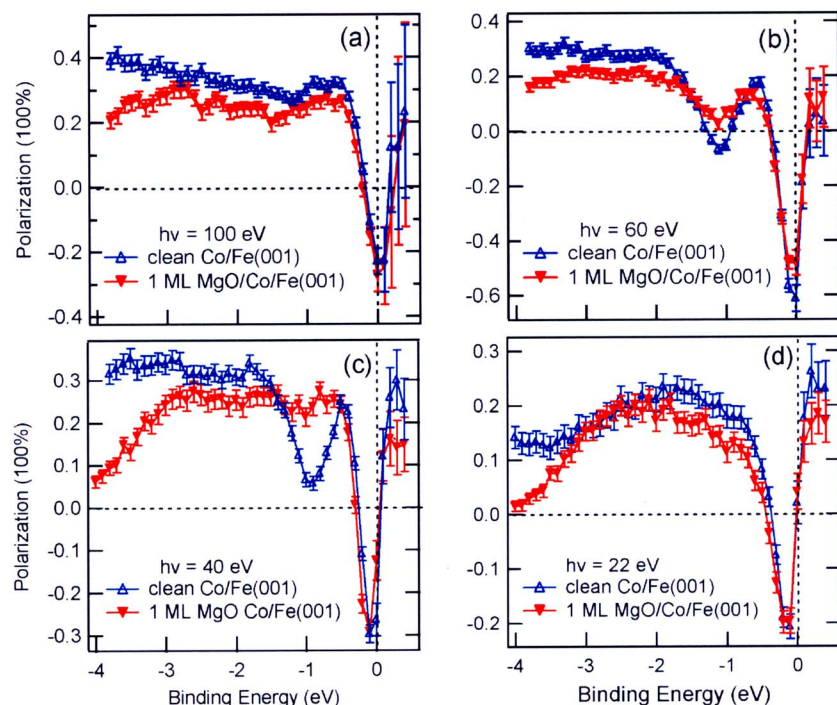


FIG. 7. (Color online) The spin polarization spectra for the sample of MgO (t_{MgO})/Co(8 ML)/Fe(15 ML)/GaAs(001) with MgO thickness $t_{\text{MgO}}=0$ and 1 ML at a photon energy of (a) $h\nu=100$ eV; (b) $h\nu=60$ eV; (c) $h\nu=40$ eV; (d) $h\nu=22$ eV, respectively.

below MgO overlayers of the MgO/Co/Fe/GaAs(001) film are almost not affected.

Figure 7 compiles the spin polarization spectra at several typical photon energies of $h\nu=22$, 40, 60, and 100 eV, respectively, for the sample of MgO (t_{MgO})/Co(8 ML)/Fe(15 ML)/GaAs(001) film with a different MgO thickness of $t_{\text{MgO}}=0$ and 1 ML. One can see that after covering the MgO overlayer on the Co/Fe/GaAs(001) surface, the spin polarization at E_F shows only a moderate decrease due to the spin-averaged scattering in nonmagnetic MgO oxide, and keeps the negative sign of the spin polarization. The negative spin polarization at the Fermi level for MgO/Co/Fe/GaAs(001) film is in contrast to the positive spin polarization observed for the MgO/Fe/GaAs(001) system.³² This different MgO effect on the sign of spin polarization of the MgO/Fe(001) and the MgO/Co/Fe(001) systems through MgO overlayer(s) could be understood by the different energy band structures at the Fermi level for bcc Fe(001) and bct Co(001). In the bcc Fe(001) case the quenching of the transitions from the minority initial states in Δ_5^\downarrow symmetry lying just below the Fermi level results in positive spin polarization at the MgO/Fe(001) interface. However, for the MgO/bct Co/bcc Fe(001) system, the Δ_5^\downarrow symmetry is shifted down about one electron voltage away from Fermi energy of bct Co(001). The quenching of transitions from Δ_5^\downarrow symmetry upon MgO overlayers does not affect the spin properties at E_F because the transitions from minority Δ_1^\downarrow symmetry dominate the density of state at Fermi level of bct Co(001), resulting in a negative spin polarization of the MgO/Co/Fe(001) at E_F as shown in Fig. 7.

The origin of the sign and magnitude of the tunneling spin polarization (TSP) from ferromagnetic metals through an oxide barrier has become a focus of recent research interest in the MTJs. There are several techniques that can be employed to measure the TSP through FM/oxide barriers, such as

Meservey and Tedrow's technique,³³ Andreev reflection method,³⁴ and spin-resolved photoemission spectroscopy. Spin-resolved photoemission gives a wavevector- and symmetry-resolved view of the spin polarization at the Fermi level. As the tunneling through the MgO barrier involves mostly electrons with $K_{\parallel}=0$, our normal emission experiments probe those states relevant for the spin-dependent tunneling. Nearly all measurements to date have reported positive TSP values including all the 3D transition-metal ferromagnets.^{33,35,36} Negative TSP has been measured only in two ferromagnetic oxides, SrRuO₃ (Ref. 37), Fe₃O₄ (Ref. 38), and has been inferred in a small number of cases from TMR studies.³⁹⁻⁴¹ Our spin-resolved photoemission spectroscopy study at the MgO/Co(001) as well as the MgO/Fe(001) interfaces suggests that the energy band structure at the Fermi level and spin dependent modification of an electron state at the FM/oxide barrier interface play a decisive role for the sign and magnitude of spin polarization of the ferromagnetic electrode through the oxide barrier.

IV. DISCUSSION AND CONCLUSION

The interpretation of the spin- and angle-resolved photoemission spectroscopy of the MgO covered Co/Fe/GaAs(001) film is much more complicated than the situation of a clean Co/Fe(001) surface. The oxide adsorption on a clean 3d metal surface normally results in an attenuation of the 3d emission. The measured spectrum is certainly a combination of initial- and final-state effects including the medial scattering process in the MgO overlayer. The effect of redistribution of electronic states upon adsorption is, of course, the one of primary interest. The recent first-principles electronic structure calculation predicts that the charge rearrangement necessary to correctly offset the bands of the MgO relative to those of Co leads to only

very little charge transfer between MgO and Co layers.¹⁶ However, a previous first-principles study on a $p(1 \times 1)$ O/Fe(001) system predicted the adsorption-induced Fe surface atoms relaxation is 23% of the Fe interlayer spacing, and this upward shift of Fe surface (as well as subsurface) layers leads to a narrowing and localization of the surface and subsurface d bands through hybridization. This upward shift also leads to a significant loss of minority electrons and consequently a large enhancement in the magnetic moments induced by Fe surface and subsurface layers.⁴² The previous theoretical predication seems to support our above experimental observation of spin and symmetry dependent attenuation of photon electrons upon the MgO overlayer.

Upon MgO overlayer(s), the observed general feature of spin and symmetry dependent modification of the electronic structure for bcc Fe(001) and tetragonally distorted bcc Co(001) surface indicates that it may be related to a common property of the bcc (001) surface. Previous band-structure calculations⁴³ showed that there is a general bcc surface state or surface resonance state (SRS) near the Fermi level, and it may originate from a nearly unperturbed d orbital extending out into the vacuum region. The surface state or SRS is in the minority spin band for Fe and Cr. This character of SRS is also in agreement with our observation of the spin and symmetry dependent attenuation of the photoelectrons originating from a minority Δ_5^1 spatial symmetry upon MgO overlayer(s). In view of the fact that the main features measured in our spin-resolved photoemission spectra could be attributed to the bulk states of the bcc Fe(001) or the tetragonally distorted bcc Co(001) based on the direct transition model, the quenched minority feature upon MgO oxides, in our opinion, may be related to a bcc (001) surface resonance state. The quenching of the bcc (001) SRS is probably due to a rearrangement of surface atoms on a bcc or bct (001) surface to fit the adjacent layer of MgO overlayer(s) through chemical bonding and then results in a spin and spatial sym-

metry dependent modification of interface electronic structure in MgO/bcc Fe(001) and MgO/bct Co(001) systems.

Finally, it is also worthy mentioning the results of the recent theoretical calculation of electronic and transport properties of the bcc Co/MgO/Co system by Zhang and Butler, *et al.*¹⁶ They predicated that one particular state with Δ_1 symmetry is able to effectively couple from the Co into the MgO while the d -like minority electrons do not tunnel efficiently. Our result is compatible with their theoretical conclusions.

In conclusion, the spin polarization of the valence band electronic states of epitaxial Co/Fe(001)/GaAs(001) and MgO/Co/Fe(001)/GaAs(001) systems are investigated by employing spin-resolved photoemission spectroscopy. The experimental results are compared with the calculated energy band structure of the bcc and bct Co(001), and discussed in the framework of the interband transition model, which allows one to ascribe the observed spectral features to bands of given spin and spatial symmetry. In contrast to the positive spin polarization observed at the MgO/Fe(001) interface, a large negative spin polarization of the electronic states at the Fermi level is observed for a MgO/Co/Fe/GaAs(001) system. Such a large negative spin polarization is attributed to the change in energy band structure at the bct Co/bcc Fe(001) interface.

ACKNOWLEDGMENTS

The authors would like to thank the BESSY staff for support during the experiments. The work is financially supported by the Deutsche Forschungsgemeinschaft through Grant No. Schn-353/12, and the Natural Science Foundation of Education Commission of Anhui Province, China (Grant No. 2005KJ037ZD). One of the authors' work (C.-G.L.) is supported by the Korea Research Foundation Grant No. KRF-2004-005-D00096.

*Corresponding author. Email address: Intong@ahut.edu.cn

¹J. S. Moodera, E. F. Gallagher, K. Robinson, and J. Nowak, *Appl. Phys. Lett.* **70**, 3050 (1997).

²S. S. P. Parkin, K. P. Roche, M. G. Samant, P. M. Rice, R. B. Beyers, R. E. Scheuerlein, E. J. O'Sullivan, S. L. Brown, J. Bucchigano, D. W. Abraham, Y. Lu, M. Rooks, P. L. Trouilloud, R. A. Wanner, and W. J. Gallagher, *J. Appl. Phys.* **85**, 5828 (1999).

³C. Vouille, A. Barthélémy, F. Elokani Mpondo, A. Fert, P. A. Schroeder, S. Y. Hsu, A. Reilly, and R. Loloee, *Phys. Rev. B* **60**, 6710 (1999).

⁴T. N. Todorov, E. Y. Tsymlal, and D. G. Pettifor, *Phys. Rev. B* **54**, R12685 (1996).

⁵D. Wang, C. Nordman, J. M. Daughton, Z. Qian, and J. Fink, *IEEE Trans. Magn.* **40**, 2269 (2004).

⁶J. L. Vassent, M. Dynna, A. Marty, B. Gilles, and G. Patrat, *J. Appl. Phys.* **80**, 5727 (1996).

⁷M. Klaua, D. Ullmann, J. Barthel, W. Wulfhelkel, J. Kirschner, R. Urban, T. L. Monchesky, A. Enders, J. F. Cochran, and B. Hei-

nrich, *Phys. Rev. B* **64**, 134411 (2001).

⁸J. Mathon and A. Umerski, *Phys. Rev. B* **63**, 220403(R) (2001).

⁹W. H. Butler, X.-G. Zhang, T. C. Schulthess, and J. M. MacLaren, *Phys. Rev. B* **63**, 054416 (2001).

¹⁰Shinji Yuasa, Akio Fukushima, Taro Nagahama, Koji Ando, and Yoshishige Suzuki, *Jpn. J. Appl. Phys., Part 2* **43**, L588 (2004).

¹¹S. S. P. Parkin, C. Kaiser, A. Panchula, P. M. Rice, B. Hughes, M. Samant, and S.-H. Yang, *Nat. Mater.* **3**, 862 (2004).

¹²X.-G. Zhang, W. H. Butler, and Amrit Bandyopadhyay, *Phys. Rev. B* **68**, 092402 (2003).

¹³H. L. Meyerheim, R. Popescu, J. Kirschner, N. Jedrecy, M. Sauvage-Simkin, B. Heinrich, and R. Pinchaux, *Phys. Rev. Lett.* **87**, 076102 (2001).

¹⁴H. Oh, S. B. Lee, Jikeun Seo, H. G. Min, and J.-S. Kim, *Appl. Phys. Lett.* **82**, 361 (2003).

¹⁵M. Sicot, S. Andrieu, P. Turban, Y. Fagot-Revurat, H. Cercellier, A. Tagliaferri, C. De Nadai, N. B. Brookes, F. Bertran, and F. Fortuna, *Phys. Rev. B* **68**, 184406 (2003).

¹⁶X.-G. Zhang and W. H. Butler, *Phys. Rev. B* **70**, 172407 (2004).

- ¹⁷G. A. Prinz, Phys. Rev. Lett. **54**, 1051 (1985).
- ¹⁸P. Houdy, P. Boher, F. Giron, F. Pierre, C. Chappert, P. Beauvilain, K. L. Dang, P. Veillet, and E. Velu, J. Appl. Phys. **69**, 5667 (1991).
- ¹⁹H. Wieldraaijer, J. T. Kohlhepp, P. LeClair, K. Ha, and W. J. M. de Jonge, Phys. Rev. B **67**, 224430 (2003).
- ²⁰P. Alippi, P. M. Marcus, and M. Scheffler, Phys. Rev. Lett. **78**, 3892 (1997).
- ²¹S. Fox and H. J. F. Jansen, Phys. Rev. B **60**, 4397 (1999).
- ²²H. Wieldraaijer, J. T. Kohlhepp, P. LeClair, K. Ha, and W. J. M. de Jonge, Phys. Rev. B **67**, 224430 (2003).
- ²³M.-H. Schaffner, F. Patthey, and W.-D. Schneider, Surf. Sci. **417**, 159 (1998).
- ²⁴Y. B. Xu, E. T. M. Kernohan, D. J. Freeland, A. Ercole, M. Tselepi, and J. A. C. Bland, Phys. Rev. B **58**, 890 (1998).
- ²⁵M. Zolfl, M. Brockmann, M. Kohler, S. Kreuzer, T. Schweinbock, S. Miethaner, F. Bensch, and G. Bayreuther, J. Magn. Magn. Mater. **175**, 16 (1997).
- ²⁶T. L. Monchesky, B. Heinrich, R. Urban, K. Myrtle, M. Klaua, and J. Kirschner, Phys. Rev. B **60**, 10242 (1999).
- ²⁷M. Madami, S. Tacchi, G. Carlotti, G. Gubbiotti, and R. L. Stamps, Phys. Rev. B **69**, 144408 (2004).
- ²⁸H. Ebert, The Munich SPR-KKR package, version 2.1, <http://olymp.cup.uni-muenchen.de/ak/ebert/SPRKKR>; H. Ebert, in *Fully Relativistic Band Structure Calculations for Magnetic Solids—Formalism and Application*, edited by H. Dreysse, Lecture Notes in Physics Vol. 535 (Springer, Berlin, 2000), p. 191.
- ²⁹L. Duo, R. Bertacco, G. Isella, F. Ciccacci, and M. Richter, Phys. Rev. B **61**, 15294 (2000).
- ³⁰S. Yuasa, T. Katayama, T. Nagahama, A. Fukushima, H. Kubota, Y. Suzuki, and K. Ando, Appl. Phys. Lett. **87**, 222508 (2005).
- ³¹F. Matthes, L.-N. Tong, and C. M. Schneider, J. Appl. Phys. **95**, 7240 (2004).
- ³²A detailed description of our study on MgO/Fe(001) system will be published elsewhere. Our result of positive spin polarization measured at MgO/Fe(001) system is in agreement with that by another group (see Ref. 15).
- ³³R. Meservey and P. M. Tedrow, Phys. Rep. **238**, 173 (1994).
- ³⁴R. J. Soulen, Jr., J. M. Byers, M. S. Osofsky, B. Nadgorny, T. Ambrose, S. F. Cheng, P. R. Broussard, C. T. Tanaka, J. Nowak, J. S. Moodera, A. Barry, and J. M. D. Coey, Science **282**, 85 (1998).
- ³⁵D. J. Monsma and S. S. P. Parkin, Appl. Phys. Lett. **77**, 720 (2000).
- ³⁶B. Nadgorny, R. J. Soulen, Jr., M. S. Osofsky, I. I. Mazin, G. Laprade, R. J. M. van de Veerdonk, A. A. Smits, S. F. Cheng, E. F. Skelton, and S. B. Qadri, Phys. Rev. B **61**, R3788 (2000); Christian Kaiser, Alex F. Panchula, and S. S. P. Parkin, Phys. Rev. Lett. **95**, 047202 (2005).
- ³⁷D. C. Worledge and T. H. Geballe, Phys. Rev. Lett. **85**, 5182 (2000).
- ³⁸A. F. Panchula, Ph.D. thesis, Stanford University, Stanford, 2003.
- ³⁹M. Sharma, S. X. Wang, and J. H. Nickel, Phys. Rev. Lett. **82**, 616 (1999).
- ⁴⁰J. M. de Teresa, A. Barthelemy, A. Fert, J. P. Contour, F. Montaigne, and P. Seneor, Science **286**, 507 (1999).
- ⁴¹C. Mitra, P. Raychaudhuri, K. Dörr, K.-H. Müller, L. Schultz, P. M. Oppeneer, and S. Wirth, Phys. Rev. Lett. **90**, 017202 (2003).
- ⁴²S. R. Chubb and W. E. Pickett, Phys. Rev. Lett. **58**, 1248 (1987).
- ⁴³J. A. Stroscio, D. T. Pierce, A. Davies, R. J. Celotta, and M. Weinert, Phys. Rev. Lett. **75**, 2960 (1995).